Available online at www.sciencedirect.com

ScienceDirect

Procedia Structural Integrity 78 (2026) 1126–1133

Structural Integrity Procedia

www.elsevier.com/locate/procedia

XX ANIDIS Conference

# Effects of Non-Structural Walls on Vertical Floor Acceleration Demands: A Case Study

Irfan Ali[a,b,*], Rola Assi[a], Giovanni Muciaccia[b]

[a]*Département of Construction Engineering, École de Technologie Supérieure (ETS), Montréal, QC H3C 1K3, Canada*

[b]*Department of Civil and Environmental Engineering, Politecnico di Milano, Piazza Leonardo da Vinci, 32, 20133 Milan, Italy*

**Abstract**

Non-structural components (NSCs) are highly susceptible to seismic damage, often driving major economic losses. This vulnerability is exacerbated in near-fault zones, where vertical ground motions can exceed horizontal components, challenging conventional NSC design approaches and amplifying safety risks. This study investigates how different non-structural wall configurations affect vertical floor acceleration demands and quantifies the corresponding demands on suspended ceilings. Linear time-history analyses were conducted on various structural models: (bare frame, full frame, two variants of masonry-wall-only frames, and one curtain-wall-only frame) using 65 strong vertical ground motions (>0.25 g). Computed $PFA_v/PGA_v$ ratios show that masonry-wall only frames with walls on lower stories significantly amplify vertical accelerations on upper floors, with mid-story peaks exceeding $3.6 \times PGA_v$. In contrast, curtain-wall-only frame exhibits more uniform responses. Roof-level amplifications remain moderate ($3.0–3.5 \times PGA_v$) across all configurations. Notably, floor level responses exhibited up to 100% variability at different nodes on the same story highlighting the impact of irregular wall distributions. Suspended ceilings experienced, on average, 20% (84thpercentile) higher vertical accelerations than their supporting floor. Based on these findings, two recommendations are proposed: (1) A baseline vertical amplification factor of $3.00 \times PGA_v$ adjusted for wall configurations and floor location; (2) A 1.20 amplification ratio for estimating suspended ceiling accelerations relative to supporting floor.



*Keywords:* Non-Structural Walls; Suspended Ceiling; Vertical Ground Motion; Vertical Floor Acceleration Demands.

* Corresponding author. Tel.: +39-348-6584986
*E-mail address:* irfan.ali@mail.polimi.it

2452-3216 
10.1016/j.prostr.2025.12.144

## 1. Introduction

Nonstructural components (NSCs) such as partitions, suspended ceilings, and cladding are typically more vulnerable to seismic action than primary structural elements, given their lower strength, limited ductility, and secondary priority in design. These NSCs can be economically critical, accounting for up to 92% of construction costs in hospital buildings construction (Taghavi and Miranda, 2003), and their failure can cause significant economic disruption, functional downtime, and life safety risks.

While seismic design traditionally emphasizes horizontal ground motion, empirical evidence from near-fault earthquakes such as the 1994 Northridge, 2009 L'Aquila, and 2016 Kaikōura events shows that vertical ground accelerations can not only exceed design assumptions but also critically contribute to NSC damage. Historical earthquakes confirm these systemic failures. For instance, the vertical to horizontal (V/H) acceleration ratio reached 1.79 in the 1994 Northridge earthquake, causing widespread ceiling collapses and punching shear failures (Bozorgnia and Campbell, 2004; Hilmy and Masek, 1994). L'Aquila (2009) saw over 60% of buildings damage and hospitals shutdowns mainly due to NSCs failure (Di Sarno et al. 2011; Alexander, 2010). The 2016 Kaikōura event recorded vertical accelerations up to 2.7 g, resulting in extensive NSC damage (Bradley et al., 2017). In near-fault regions the vertical component of ground motion can dominate, especially under high V/H ratios exceeding 1.0 and pulse-like excitations, yet current codes (e.g., ASCE 7, NBC 2015) often oversimplify vertical demands with fixed V/H factors and rigid diaphragm assumptions (Mazloom, 2023; Mazloom and Assi, 2023; Assi et al., 2016).

These simplifications neglect several key phenomena: (i) the amplification of vertical floor accelerations in flexible floor systems; (ii) the dynamic interaction between NSCs and their supporting structure; and (iii) the contribution of NSC stiffness and mass to overall system dynamics. As a result, design peak floor accelerations (PFAs) are commonly underestimated particularly for acceleration-sensitive NSCs like suspended ceilings leading to repeated and costly failures (Dhakal et al., 2011; FEMA, 2011).

Despite these concerns, few parametric studies have examined how variations in NSC mass and stiffness influence vertical acceleration amplification ($PFA_v/PGA_v$), and no widely accepted methodologies currently exist to estimate the vertical acceleration demands imposed on suspended ceilings relative to their supporting floor. Instead, design practices typically apply uniform amplification factors, disregarding the role of infill configurations, floor flexibility, and local structural characteristics.

This study addresses these gaps by investigating vertical acceleration amplification in a representative case study building. Using vertical ground motions, it evaluates the $PFA_v/PGA_v$, ratios across floor levels for different structural configurations to assess how Non-Structural Walls (NSWs) affect vertical floor acceleration demands. Furthermore, it estimates the acceleration demands imposed on suspended ceiling (SC) relative to their supporting floor. Based on these findings, an empirical and configuration-specific framework is developed to interpret vertical floor amplification and ceiling demands, offering guidance for evaluation of vertical demands for NSCs in near-fault environments.

## 2. Methodology

This study employs a finite element (FE) based assessment to investigate the influence of Non-Structural Walls on vertical floor acceleration demands, using the La Maison des Étudiants (MDE), a five-story reinforced concrete (RC) building located in Montreal, Canada, as a case study. Finite element analysis was conducted using ETABS. The Five FEM models utilized in this study are based on the work of (Assi and Ramadan, 2022), who calibrated them using ambient vibration measurements (AVMs) to accurately match the natural periods of both the Bare and Full frame models, thereby capturing the dynamic behaviour of the structures.The structural system consists of RC cores and columns with slabs and beams with 35 MPa concrete. The building features an irregular geometry that enables the analysis of spatial variations and nonuniform amplification of vertical acceleration. NSCs integrated within the

structure include approximately 1,740 m² of masonry walls and 3,726 m² of curtain walls, allowing for comparative analysis across different façade and partition configurations.

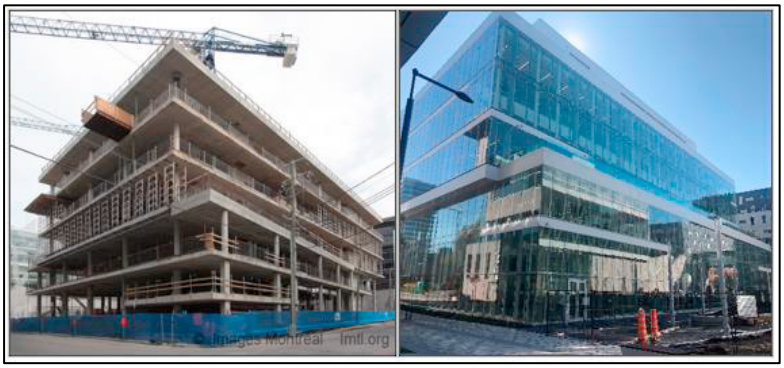

Fig. 2.1 Case Study Building Photo (MDE). Source: Ramadan, 2022.

Five structural configurations were analysed to assess the impact of NSWs on floor level vertical acceleration demands: (1) a Bare Frame including only the structural elements , (2) a Full Frame incorporating both masonry and curtain walls, (3) a Masonry Walls configuration with walls up to the second floor, (4) a Masonry Walls configuration with walls up to third floor, (5) a Curtain Walls only model. The five models are shown in Fig 2.2.

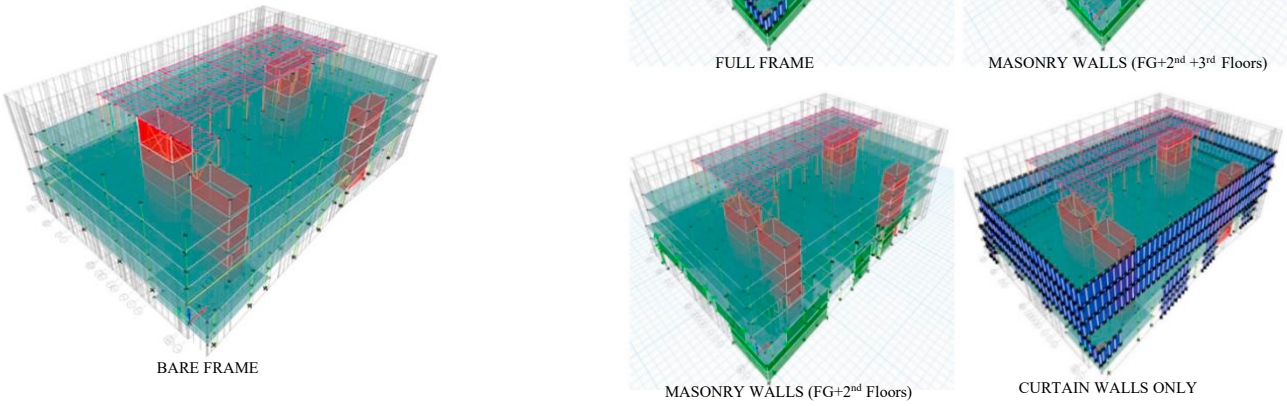


Figure 2.2 Parametric FEM Models

To assess vertical acceleration demands of suspended ceiling, a separate Bare Frame configuration was analysed by modelling a suspended ceiling using floating system as shown in Fig 2.3. The suspended ceiling was simulated using gypsum panels connected by tension-only hangers placed below the roof slab. The properties of the suspended ceiling panel are reported in Table 2.1.

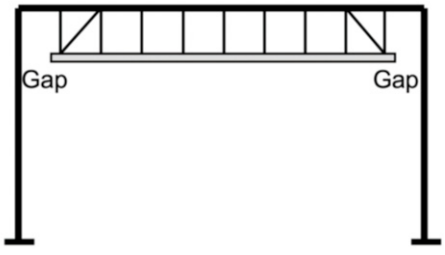


Figure 2.3 Floating Suspended Ceiling

Table 2.1 Properties of Suspended Ceiling

| Component | Parameter | Value | Units | Comments |
|---|---|---|---|---|
| Suspended Ceiling | Material | Gypsum | - | Typical gypsum board material |
| | Modulus of Elasticity | 600 | $MPa$ | Represents the stiffness of the gypsum |
| | Mass Density | 600 | $kg/m3$ | Standard density for gypsum |
| | Poisson's ratio | 0.2 | - | Typical value for gypsum |
| | Thickness | 10 | $mm$ | Governs flexural behavior |
| | Applied load | 0.196 | $kN/m2$ | Represents the dead load |

Linear Time history analysis was conducted using a suite of 65 near-fault vertical ground motion records (5.5 < MW < 8.0; 0.0 < $R_{rup}$ <25 km and $PGA_v$ > 0.25 g) selected for Site Class C conditions (VS30 = 360–760 m/s); source of the data (Mazloom,2023). A Rayleigh damping ratio of 5% was used. In modelling assumptions, linear elastic material behaviour was adopted, with no soil–structure interaction (fixed-base support) and no rigid diaphragm assumptions, allowing floor flexibility to be accurately captured. The suspended ceiling model included gypsum panels supported by tension-only hangers (k = 33.7 $kN/m$), with no assumed composite action with the floor slab.

## 3. Results and Discussion

### 3.1 Effect of Non-Structural Walls on Floor Acceleration Demands

As illustrated in the process diagram Figure 3.1, peak floor accelerations ( $PFA_v$ ) were extracted at critical nodes across the structure, and $PFA_v/PGA_v$ ratios were computed for each model. $PFA_v$ values were extracted at mid slab panels for three vertically aligned nodes (S1, S2, S3) per floor, Fig 3.2 shows plane view of 2nd floor. The location of nodes was based on: (i) the building's irregularity, which required mid-slab panel placement to maintain vertical alignment across floors; (ii) prior research by (Mazloom, 2023) indicating that nodes at the center of slab panels experience peak acceleration demands; and (iii) the expectation that mid-slab regions would capture critical dynamic response. $PFA_v/PGA_v$ amplification ratios were statistically analysed (16th, median, 84th percentiles). The 84th percentile values (representing upper-bound demands) were plotted against normalized building height to assess NSW location/type effects on amplification.

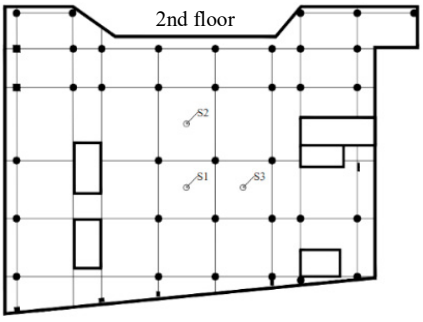


Figure 3.2 Plan view of 2nd Floor for case study

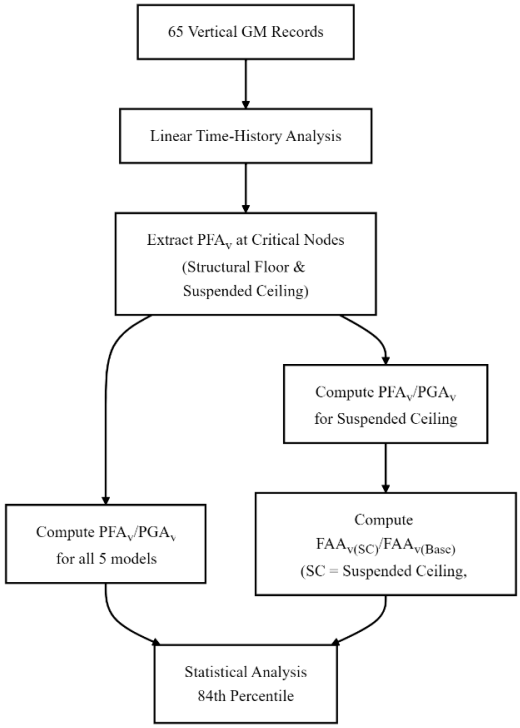


Figure 3.1 Workflow for Vertical Ground Motion Analysis and $PFA_v$ Based Result Extraction

As The results show that the 84th percentile $PFA_v/PGA_v$ ratios vary significantly with NSW configuration. At the roof ($h_{norm}$ = 1.0); where $h_{nom}$ is normalised height of the building, the Bare Frame configuration yields a maximum amplification of 3.16 $PGAv$ at the mid-slab node (S1). When only Masonry walls are present, the highest amplification is observed, reaching around 3.42 $PGAv$, while Curtain walls alone result in the amplification, at approximately 1.84

$PGAv$. At mid-height levels ($h_{nom} \approx 0.4$–$0.8$), the Bare frame shows amplifications ranging from 2.17 to 3.35 $PGAv$. The Curtain wall configuration displays the most uniform response, with amplification values smoothing out at around 2.92 $PGAv$, as shown in Fig 3.5. In contrast, Masonry only configurations as shown in Fig: 3.3 and 3.4 produce pronounced "S-shaped" amplification profiles at mid stories, with peaks occasionally exceeding 3.60 $PGAv$.

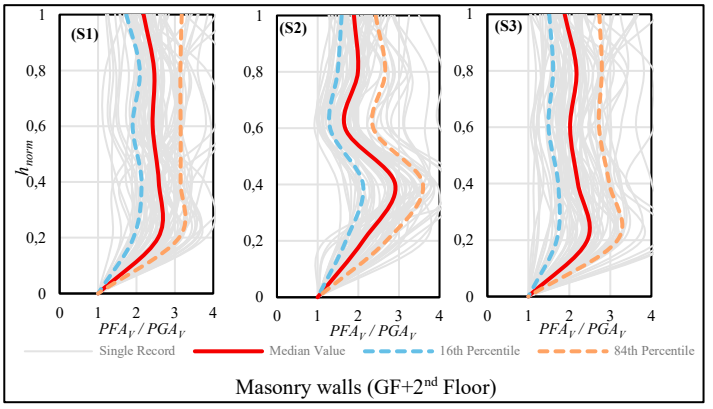


Figure 3.3 $PFAv/PGAv$ profiles of Masonry walls (GF+2nd Floor)

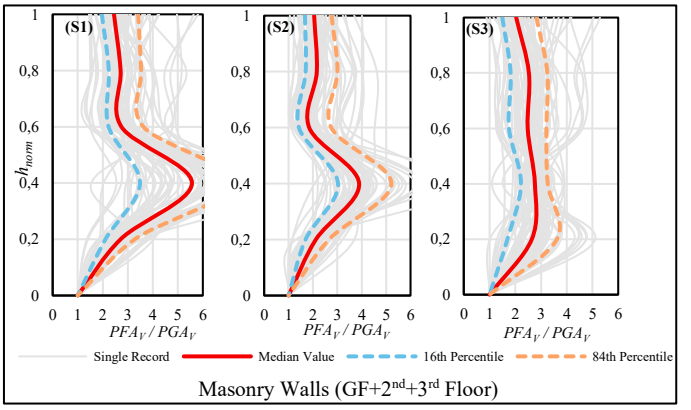


Figure 3.4 $PFAv/PGAv$ profiles of Masonry walls (GF+2nd+3rd Floor)

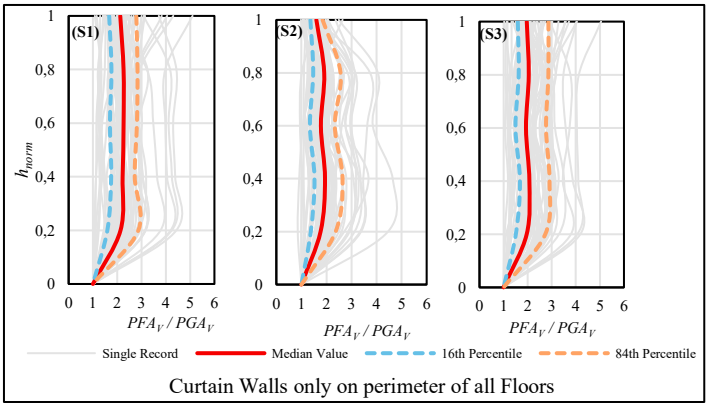


Figure 3.5 $PFAv/PGAv$ profiles of Curtain Walls only

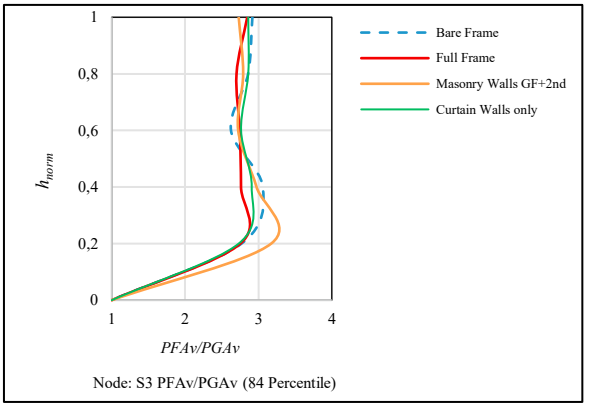


Figure 3.6 Comparison of $PFAv/PGAv$ profiles of all five models

Significant intra-floor variability in $PFA_v/PGA_v$ was observed across nodes (S1, S2, S3) in all models. At the roof level, S1 consistently showed the highest amplification. For example, in the Bare frame, S1 was approximately 18% higher than S2 and 8% higher than S3. In the Curtain walls configuration, S1 exceeded S2 by 55%. The presence of Masonry walls on the ground and second floors further increased this disparity, with S1 amplifications up to 31% higher than S2. At mid-height story levels, amplification differences across nodes ranged from 12% to 33%, depending on the model.

### 3.2 Acceleration Demands of Suspended Ceiling

Vertical acceleration demands on the suspended ceiling (SC) were computed using the Bare frame model subjected to 65 vertical ground motions, providing baseline demands unaffected by NSWs. The suspended ceiling was modelled 200 mm below the supporting slab and connected via tension-only links. To evaluate amplification, the vertical Accelerations, at three centrally located nodes (S1, S2 and S3) as illustrated in Fig 3.7, were compared against those of the supporting slab (Baseline). The 84th percentile values of $PFA_v/PGA_v$ of suspended ceiling were used for comparison, with results summarized in Table 3.1. For the suspended ceiling, the ratio of ceiling to floor acceleration $FAA_{v(SC)}/FAA_{v(Base)}$ was evaluated to capture amplification with respect to supporting floor. Where $FAA_{v(SC)}$ is $PFA_v/PGA_v$ of suspended ceiling and $FAA_{v(Base)}$ is $PFA_v/PGA_v$ of supporting floor.

Table 3.1 Statistical Distribution of $PFA_v/PGA_v$ for Suspended Ceiling (SC) and Floor (Baseline)

| Node: | Scenario | Median | Percentile 16th | Percentile 84th |
|---|---|---|---|---|
| S1 | Baseline | 2.35 | 1.80 | 3.16 |
| | SC | 2.20 | 1.85 | 2.93 |
| S2 | Baseline | 2.04 | 1.58 | 2.67 |
| | SC | 2.20 | 1.75 | 3.15 |
| S3 | Baseline | 1.98 | 1.61 | 2.92 |
| | SC | 2.21 | 1.77 | 2.94 |

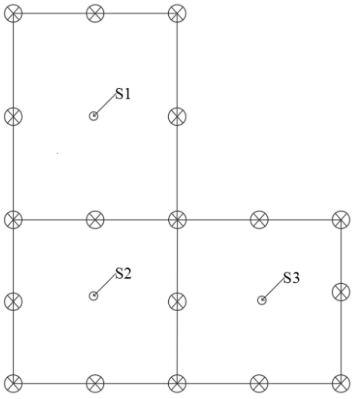


Figure 3.7 Plan view of Suspended Ceiling panel with selected nodes

A Statistical analysis was conducted to quantify the vertical acceleration amplification of suspended ceilings (SC) relative to their supporting floor slabs. This was achieved by calculating the ratio of their respective acceleration demands ($PFA_v/PGA_v$). This ratio is defined as $Amp_{(SC)} / Amp_{(Base)}$; where $Amp_{(SC)}$ is $PFA_v/PGA_v$ for the ceiling and $Amp_{(Base)}$ $PFA_v/PGA_v$ for the floor. Analysis across three nodes revealed distinct behaviors.


Figure 3.8 Ratio $of\ PFAv/PGAv$ of Suspended Ceiling to Supporting Floor (Baseline) (Node: S1, S2 and S3)

Node S1 exhibited minimal variability, with amplification ratios tightly clustered around 1.0 (range: 0.80-1.12), a mean of 0.96, a standard deviation of 0.06-0.07, and an 84th percentile ratio of 1.024, indicating only a 2.4% increase relative to the supporting floor. In contrast, Nodes S2 and S3, as shown in Fig 3.8, displayed significantly greater fluctuations. Node S2 showed a wider range of 0.53-1.79, a mean of 1.07, a standard deviation of approximately 0.30, and an 84th percentile ratio of 1.27, corresponding to a 27% increase. Node S3 had a range of 0.53-1.70, a mean of 1.05, a standard deviation of 0.25-0.30, and an 84th percentile ratio of 1.28, indicating a 28% increase. Based on the 84th percentile values across all nodes, the suspended ceiling experienced a maximum vertical acceleration amplification of approximately 30%, with an average increase of about 20% compared to the supporting floor.

### 3.3 Proposed Estimation of Peak Floor Acceleration due to Non-Structural Walls (NSWs)

An empirical and configuration-specific framework is proposed for estimating peak floor acceleration ($PFA$) due to non-structural walls (NSWs), which begins with a global baseline vertical amplification factor of 3.00 $PGAv$ (denoted as $VA_{v,global}$) for a typical six-story reinforced concrete frame, consistent with literature and experimental results as studied by (Mazloom, 2023), showing a roof-level 84th-percentile $PFAv/PGAv$ of approximately 3.16. This baseline applies to structures analyzed with linear time history under specific conditions: strong vertical earthquakes ($Mw > 5.5, Site\ Class\ C, Rrup < 25\ km,\ PGAver > 0.25g$), without dissipation sources.

Different NSW configurations modify the vertical floor acceleration demands as observed in this study. These effects are captured by a configuration factor ($\alpha_{config}$). For Masonry walls only on lower floors, $\alpha_{config}$ ranges from 1.10 to 1.20 due to significant mid-floor spikes (exceeding 3.60 $PGAv$). For Curtain walls Only, $\alpha_{config}$ is 1.00, associated with lower amplification (~2.79×$PGAv$). For The Full Frame (Masonry + Curtain), $\alpha_{config}$ is equal to 1.07, showing moderate amplification due to partial counterbalancing between Curtain and Masonry. The Bare Frame retains $\alpha_{config} = 1.0$.

To account for height-dependent effects, the building is divided into three vertical zones based on infill wall distribution: Zone A includes the infilled floors, Zone B consists of the transition floors located directly above the infilled stories, and Zone C represents the roof and uppermost levels. A zone-specific correction factor, denoted as $\beta$zone, is applied to capture the localized influence of wall discontinuities on vertical acceleration demands. For Zones A and C, $\beta$zone =1.0, indicating no additional amplification beyond the global baseline. In contrast, Zone B, particularly in configurations with masonry walls, exhibits intensified vertical acceleration due to abrupt stiffness changes, with βzone values ranging from 1.5 to 1.7. This elevated factor accounts for observed amplification peaks reaching as high as 5.4 to 6.0 × $PGA_v$.

The final acceleration estimate is given in Equation 1:

$$VA_{v,global} = 3.00 \times \alpha_{config} \times \beta_{zone} \times \text{PGAv} \quad (1)$$

$\beta_{zone}$=1.0 for Zones A and C, $\beta_{zone} \in$ [1.5,1.7] for Zone B.

### 3.4 Proposed Estimation of Vertical Acceleration of Suspended Ceiling

For suspended ceilings, acceleration demands ($PFAv/PGAv$) relative to the supporting floor are quantified by a modification factor:

$$F = \frac{PFA_{v,FC}}{PFA_{v,Baseline}};\quad F = \frac{PFA_{v,FC}}{PFA_{v,Baseline}} \cong \begin{cases} 1.02 \ldots . (S1) \\ 1.27 \ldots . (S2) \\ 1.28 \ldots . (S3) \end{cases} \qquad \text{F} \in [1.02\text{-}1.28] \quad (2)$$

Final adjustment:

$$F = \frac{PFA_{v,FC}}{PFA_{v,Baseline}} \cong 1.20 \quad (3)$$

Based on 84th-percentile values across three nodes, F ranges from 1.02 (minimal 2% increase) to 1.28 (28% amplification), with an average of 1.20. A conservative factor of F ≈ 1.20 is recommended, indicating suspended ceilings experience ~20% higher vertical accelerations on average than their supporting floor.

### 4. Conclusion

Linear time history analysis reveals significant variability in vertical floor acceleration demands, with 84$^{th}$ percentile $PFA_v/PGA_v$ ratios ranging from 1.96 to 3.28 $PGAv$ across different wall configurations. Node-specific differences

exceeding 50% at identical floors highlight the critical influence of local factors like slab geometry and mass distribution. Masonry walls on lower floors induce pronounced mid-level amplification spikes exceeding 3.60 $PGAv$, while curtain walls yield more uniform responses. Furthermore, suspended ceilings consistently experience amplified acceleration, averaging 20% higher than those of their supporting floors in terms of 84$^{th}$ percentile. To address these findings, two simplified empirical and configuration-specific frameworks are proposed: first, a baseline amplification factor of 3.00× $PGAv$ for floors, adjustable via configuration-specific and zone-dependent corrections to capture local dynamic effects; second, a direct 1.20 amplification ratio for estimating suspended ceiling accelerations relative to supporting floors. These approaches provide an empirical framework to quantify vertical acceleration demands. Future parametric studies should refine configuration-specific interactions of non-structural walls and investigate connection properties of suspended ceilings to accurately sees the acceleration demands and thereby enhance seismic resilience of acceleration-sensitive non-structural components.

## References


Alexander, D. "The L'Aquila earthquake of 6 April 2009 and Italian government policy on disaster response." Journal of Natural Resources Policy Research, vol. 2, no. 4, pp. 325–342, 2010. doi:10.1080/19390459.2010.511450.

Bradley, Brendon & Razafindrakoto, Hoby & Polak, Viktor. (2017). Ground-Motion Observations from the 14 November 2016 Mw 7.8 Kaikoura, New Zealand, Earthquake and Insights from Broadband Simulations. Seismological Research Letters. 88 10.1785/0220160225.

Dhakal, R. P., MacRae, G. A., & Hogg, K. (2011). Performance of Ceilings in the February 2011 Christchurch Earthquake. Bulletin of the New Zealand Society for Earthquake Engineering.

Di Sarno, L., et al. (2011). Performance of non-structural elements during the L'Aquila earthquake. Journal of Earthquake Engineering. 86.

FEMA E74 (2011). "Reducing the Risks of Non-Structural Earthquake Damage – A Practical Guide". Washington D.C., USA.

N. M. Newmark and W. J. Hall, Earthquake Spectra and Design. Berkeley, CA: Earthquake Engineering Research Institute, 1982.

R. Assi, A. Ramadan. 2022 Assessment of the effects of non-structural walls (NSWs) on the dynamic properties and interstory drifts of a case study building. Proceedings of the Fifth International Workshop on Seismic Performance of Non-Structural Elements (SPONSE) (Palo Alto, CA, USA, Dec. 05-07, 2022) Applied Technology Council.

R. Assi, S. Youance, A. Bonne, and M.-J. Nollet, "Effect of Non-Structural Components on the Modal Properties of Buildings Using Ambient Vibration Testing," in *Resilient Infrastructure*, June 1–4, 2016.

R. Brincker, L. Zhang, and P. Andersen, "Modal identification of output-only systems using frequency domain decomposition," Smart Materials and Structures, vol. 10, no. 3, pp. 441–445, 2001.

R. K. L. Su, J. Cheng, and E. S. S. Li, "Influence of non-structural components on lateral stiffness of tall buildings," The Structural Design of Tall and Special Buildings, vol. 14, no. 2, pp. 107–130, 2005.

S. I. Hilmy and J. P. Masek, 'Failure mechanisms of parking structures damaged during the Northridge earthquake, January 17, 1994', Special Report, Dames & Moore Structural/Earthquake Engineering Group, June 1994.

S. Mazloom, Evaluation of Vertical Ground and Floor Accelerations and Spectra in Elastic RC Frame Buildings Located in Eastern Canada, Ph.D. dissertation, École de Technologie Supérieure, Université du Québec, Montreal, Canada, May 12, 2023.

S. Mazloom and R. Assi, "Impact of vertical ground accelerations on nonstructural components," *Substance ÉTS*, Jan. 23, 2023. [Online]. Available: https://www.etsmtl.ca/en/news/impact-of-vertical-ground-accelerations-on-nonstructural-components.

S. Taghavi and E. Miranda, "Response Assessment of Nonstructural Building Elements," *PEER Report 2003/05*, Pacific Earthquake Engineering Research Center, College of Engineering, University of California, Berkeley, 2003.

Wieser et al., "Impact of relative building height, ductility levels, and out-of-plane floor flexibility on vertical accelerations," Study on a 3-story hospital and three office buildings (3, 9, and 20 stories) with steel moment-resisting frames, 2012.

Y. Bozorgnia and K. W. Campbell, "The vertical-to-horizontal response spectral ratio and tentative procedures for developing simplified V/H and vertical design spectra," *Journal of Earthquake Engineering*, vol. 8, no. 2, pp. 175–207, 2004.